Applied Physics Letters

Mid-infrared electroluminescence from type-II In(Ga)Sb quantum dots

Cite as: Appl. Phys. Lett. **116**, 061103 (2020); https://doi.org/10.1063/1.5134808
Submitted: 06 November 2019 . Accepted: 01 February 2020 . Published Online: 11 February 2020

Andrew F. Briggs, Leland J. Nordin, Aaron J. Muhowski, Priyanka Petluru, David Silva, Daniel Wasserman, and Seth R. Bank

View Online Export Citation CrossMark

ARTICLES YOU MAY BE INTERESTED IN

A semiconductor topological photonic ring resonator
Applied Physics Letters **116**, 061102 (2020); https://doi.org/10.1063/1.5131846

Deep ultraviolet monolayer GaN/AlN disk-in-nanowire array photodiode on silicon
Applied Physics Letters **116**, 061104 (2020); https://doi.org/10.1063/1.5135570

Progress, challenges, and perspective on metasurfaces for ambient radio frequency energy harvesting
Applied Physics Letters **116**, 060501 (2020); https://doi.org/10.1063/1.5140966

© 2020 Author(s).

Applied Physics Letters ARTICLE scitation.org/journal/apl

Mid-infrared electroluminescence from type-II In(Ga)Sb quantum dots

Cite as: Appl. Phys. Lett. **116**, 061103 (2020); doi: 10.1063/1.5134808
Submitted: 6 November 2019 · Accepted: 1 February 2020 ·
Published Online: 11 February 2020

View Online Export Citation CrossMark

Andrew F. Briggs,[a] Leland J. Nordin, Aaron J. Muhowski, Priyanka Petluru, David Silva, Daniel Wasserman, and Seth R. Bank[b]

AFFILIATIONS

Microelectronics Research Center and ECE Department, The University of Texas at Austin, 10100 Burnet Rd., Bldg. 160, Austin, Texas 78758, USA

[a]abriggs@utexas.edu
[b]sbank@ece.utexas.edu

ABSTRACT

There exists significant interest in the demonstration and development of alternative mid-infrared emitters, with future applications for thermal scene projection, low-cost infrared sensing, and possible long-wavelength quantum communication applications. Type-II In(Ga)Sb quantum dots grown in InAs matrices have the potential to serve as a viable material system for wavelength-flexible, mid-infrared sources. Here, we dramatically expand the range of potential applications of these mid-infrared quantum emitters through the demonstration of surface-emitting electrically pumped mid-infrared light-emitting diodes with active regions utilizing type-II In(Ga)Sb quantum dots. Two device structures were studied, the first iteration being a single In(Ga)Sb insertion layer within a simple PIN structure and the second being a design engineered for improved room temperature emission with the addition of lattice matched AlAsSb cladding at the anode to block electrons and five layers of In(Ga)Sb dots to increase the effective volume of active material. Samples were grown by molecular beam epitaxy and the electrical and optical properties for each design were characterized as a function of temperature.

Published under license by AIP Publishing. https://doi.org/10.1063/1.5134808

The mid-infrared (mid-IR, 2–20 μm) wavelength range is of significant technological importance for applications ranging from communication and sensing to defense and security as well as for fundamental scientific investigations. Two atmospheric absorption bands within the mid-IR, the mid-wave IR (MWIR, 3–5 μm), and the long-wave IR (LWIR, 8–12 μm), offer opportunities for free-space optical communication, thermal scene projectors, and multiple sensing applications. Many of these applications require efficient, compact, wavelength-flexible, and room temperature light sources.

Rapid advancement in quantum cascade laser (QCL) technology has offered solutions for many MWIR and LWIR applications.[1,2] However, QCLs struggle to efficiently produce light at the short-wavelength side of the MWIR due to limits imposed by conduction band offsets and strain accumulation[3] and have limited efficiency when operated below threshold.[4] Interband cascade lasers (ICLs) are an attractive alternative to QCLs for mid-IR applications between 3–6 μm and have demonstrated significantly lower threshold current densities than their intersubband counterparts allowing for the potential of mid-IR LEDs.[5–9] Both variants of the cascade laser require complex designs and involved growths to achieve quantum engineered active regions of sufficient thickness to allow for lasing or efficient mid-IR emission. Type-I semiconductor lasers and LEDs are the traditional approach for achieving efficient emission at visible to near-IR wavelengths,[10] but they are hampered by Auger recombination as emission wavelength increases.[11] Band-engineering, particularly introducing quantization and the application of very high strain levels, can be used to further mitigate Auger effects while extending emission wavelength.[12–14] However, the application of strain and band structure engineering places intrinsic limitations on the material thickness and alloy compositions of such emitters.

A compromise between the complexity of a cascade laser and the intrinsic limitations of a type-I heterojunction is a diode device leveraging active regions with type-II transitions. A type-II offset between two semiconductors results in a band alignment where the conduction and valence bands of the first semiconductor sit, in energy, both above or both below the corresponding conduction and valence bands of the second semiconductor. If the bandgaps of the two semiconductors do not overlap, the alignment is referred to as "broken gap" type-III, whereas if some portion of the bandgaps overlap, the alignment is described as "staggered gap" type-II. Using such type-II

Published under license by AIP Publishing

active regions embedded in conventional PIN-junctions, LEDs, and lasers have been demonstrated with high wall-plug efficiencies at low current, suggesting decreased Auger recombination compared to bulk narrow bandgap type-I emitters while spanning a large portion of the mid-IR.[15–18] Auger recombination rates are argued to decrease with the additional quantization of energy states resulting from heterostructured emitters such as the type-II superlattice LEDs.[12,13,19,20] Increased dimensionality of quantization, moving from a heterostructure to a quantum dot, allows for quenching of Auger recombination. The potential benefits of 3D quantized structures for optoelectronic applications, first suggested by Arakawa and Sakaki,[21] have largely been experimentally explored in In(Ga)As self-assembled quantum dots (SAQD) grown compressively strained on (Al)GaAs, although SAQDs have also been demonstrated in a range of other material systems with similar lattice mismatches.[22] Such quantum structures provide a zero-dimensional density of states which leads to increased radiative transition rates and the aforementioned decrease in Auger recombination rates.[23–27] There has been some effort in recent years to utilize type-II QDs for mid-IR source applications, leveraging the benefits associated with QDs and type-II systems to access far longer wavelengths.[17] More recently, work in this In(Ga)Sb material system demonstrated approaches to engineer the carrier lifetime of mid-IR emitters.[28]

In this work, we demonstrate an electrically pumped device based on In(Ga)Sb quantum dots grown in InAs matrices with emission in the mid-IR. The results from a temperature-dependent photoluminescence (PL) study were used to design the final device active region. While the initial electrically pumped single-layer In(Ga)Sb device did not achieve strong room temperature emission, we modified the device design to be similar to PL samples that did show room temperature emission. Because of the wavelength flexible emission and robust temperature performance, In(Ga)Sb quantum emitters offer a promising alternative for room temperature, electrically pumped emission in the mid-IR.

Samples were grown in a Varian Gen. II solid-source molecular beam epitaxy (MBE) system equipped with valved-crackers for arsenic and antimony, SUMO effusion sources for gallium, indium, and aluminum, and individual dopant sources for silicon and beryllium. All growth temperatures were measured by blackbody thermometry with a kSA BandiT system. The In(Ga)Sb structures were grown with the optimal group-III ratio, Sb overpressure, and at the optimal temperature determined in previous works, which resulted in QD layers with a reported dot density of 1×10^9 cm^{-2}.[28]

In(Ga)Sb has a type-II band alignment with InAs, which results in a strong confinement for holes [in the In(Ga)Sb] but not for electrons (in the surrounding InAs).[28] This lack of electron confinement can weaken emission, specifically at higher temperatures. Lattice-matched barriers of $AlAs_{0.16}Sb_{0.84}$, which have a significant conduction band offset with InAs but minimal valence band offset, were added as an electron barrier to both confine electrons to the device active region and mitigate parasitic surface recombination. To test the effectiveness of AlAsSb confinement layers, the PL emission of two otherwise identical In(Ga)Sb samples with and without AlAsSb layers was compared. Emission scaling was studied by comparing samples containing one, three, and five layers of QDs sandwiched between AlAsSb barriers. The total amount of InAs between the AlAsSb barriers was held constant. Unlike the LED samples, these PL structures had QDs layers grown close to the sample surface to facilitate optical pumping.

The LED structures consisted of In(Ga)Sb QD active regions placed in a PIN doped InAs structure. The first device, shown in Fig. 1(a), consisted of a single In(Ga)Sb layer in the intrinsic (i) region of the InAs PIN diode. First the 550 nm n-InAs layer (n-doped to 1×10^{18} cm^{-3}) was grown, followed by a 500 nm intrinsic region with a single layer of In(Ga)Sb grown in the center. Above this was grown a 1 μm thick p-type InAs layer (doped 1×10^{18} cm^{-3}). The device was then capped with 350 nm of p$^+$ InAs doped 1×10^{19} cm^{-3} designed to serve as a current-spreading contact layer.[29] The second device, shown in Fig. 1(b), used the same basic diode structure as the first, but included five layers of In(Ga)Sb, spaced by 50 nm of InAs, and replaced the p-doped InAs with a 500 nm p-doped AlAsSb electron blocking layer doped 1×10^{18} cm^{-3}. The device was capped with a 100 nm p$^+$ InAs current spreading and contact layer. Both devices were grown on n-doped InAs substrates. Composition of the In(Ga)Sb

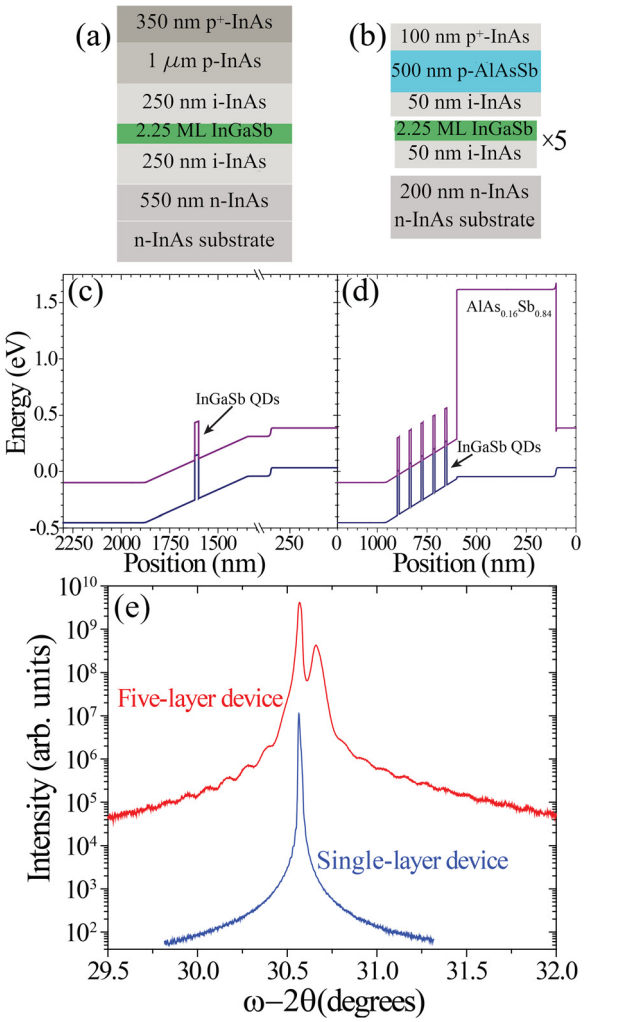

FIG. 1. Layer structure (a) and band diagram (c) of the single-layer In(Ga)Sb QD LED. (b) Layer structure and (d) band diagram of five-layer In(Ga)Sb QD LED with AlAsSb electron confinement layer. (e) X-ray diffraction $\omega - 2\theta$ scan for single-layer (blue) and five-layer (red) LED structures.

Published under license by AIP Publishing

dots and AlAsSb barriers was determined by XRD. Figure 1(e) shows the XRD spectrum from both the single- (blue) and five- (red) layer devices. The five-layer device XRD shows a crystalline AlAsSb peak and thickness fringes due to the multiple In(Ga)Sb layers in the intrinsic region of the device. The PIN-junction device samples were processed using traditional UV photolithography, wet-etch, metallization, and lift-off techniques to form LED mesas (700 μm × 600 μm).

Figure 2 shows the temperature-dependent PL spectra from the (a) single-layer sample without barriers and the (b) five-layer PL sample with conduction band barriers. In the PL at low temperature, both samples exhibited strong InAs band edge emission (at 3 μm) and then broad, weaker emission from the In(Ga)Sb QD layer(s) at 5 μm. For both samples, the InAs band edge emission decreased significantly with increasing temperature, exhibiting an 50× decrease in peak intensity as temperature was increased from 77 K to 300 K. The PL peak associated with In(Ga)Sb emission in the single-layer sample without barriers showed a similar decrease in emission intensity. The barrier sample, on the other hand, showed a decrease in peak emission intensity of less than an order of magnitude, suggesting that the addition of the conduction band barriers prevented the diffusion of electrons from the five QD layers and improved temperature performance of the QD emitters. Figure 2(c) plots the integrated PL intensity from each of the four PL samples as a function of temperature, where emission from only the spectral feature associated with QD emission was considered. The data in Fig. 2(c) reinforce the results from the temperature-dependent PL spectra. We observed the strongest emission from the five-layer sample with barriers and a decrease of only a factor of 5× as temperature was raised from 77 K to 300 K. All of the barrier samples (one, three, and five layers of QDs) behaved similarly in this regard, while the single-layer sample without barriers showed over an order of magnitude decrease in integrated emission over the temperature range studied. In addition, while the barrier samples showed a marginal increase in emission as QD layers were added, the sample without barriers had slightly stronger emission (at low temperature) than all but the five-layer barrier sample. The slight improvement in low temperature emission from the single-layer QD sample without barriers was likely a result of the weaker optical pumping efficiency of the barrier samples as the conduction band barriers (i) push the QD emitters farther from the surface (where photo-excitation of electron hole pairs (EHPs) is highest) and (ii) may block EHPs generated outside the barriers from diffusing to the emitters. Because the five-layer In(Ga)Sb PL sample with carrier blocking layers had the best temperature performance, that active region design was incorporated into the final device.

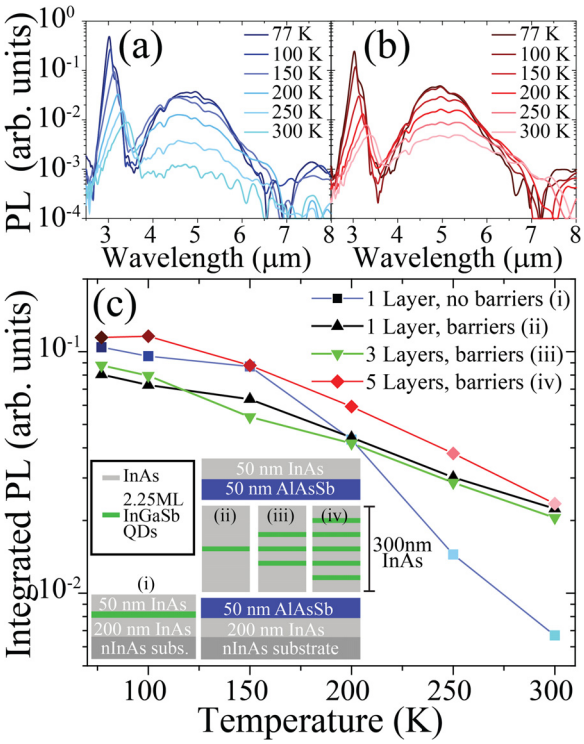

FIG. 2. Temperature-dependent PL spectra from (a) single-layer QD sample without any AlAsSb blocking layers and (b) five-layer QD sample with AlAsSb conduction band blocking layers. (c) Integrated PL as a function of temperature from single-layer QD emitters without AlAsSb blocking layers (blue) and single QD layer (black), 3 QD layer (green), and five QD layer (red) emitters with AlAsSb blocking layers. Insets: layer structures for the four PL samples.

The addition of barriers clearly improved the temperature performance of the In(Ga)Sb emitters; thus, one might expect similar benefit to the temperature performance of In(Ga)Sb QD electroluminescence (EL) devices. Of course, for our LEDs, only a single barrier was used in the device design [as shown in Fig. 1(b)], placed to limit diffusion of injected minority electrons into the p-type InAs, and thus away from the In(Ga)Sb QDs. Figure 3 shows the EL spectra from the two mid-IR LEDs. The EL spectra from the single-layer LED, shown in Fig. 3(a), were dominated by the InAs band edge feature, suggesting that significant recombination occurs in the InAs, and not the QD layer. Moreover, we observed a striking decrease in emission intensity with increasing temperature, commensurate with the results observed in the PL study shown in Fig. 2. On the other hand, the five-layer QD emitter with the AlAsSb barrier [Fig. 3(b)] showed negligible InAs band edge emission, suggesting that the majority of injected carriers recombine in the QDs, and not the InAs diffusion regions. We also observed significantly stronger room temperature emission from the five-layer QD sample with the AlAsSb barrier. The improvement in temperature performance between the two LEDs more closely resembles the improvement observed in the PL samples with the addition of the AlAsSb carrier blocking layers, with an order of magnitude increase in integrated PL intensity at elevated temperatures, than the changes observed in the PL samples with increasing layers of In(Ga)Sb [Fig. 2(c)]. Therefore, we primarily attribute the stronger room temperature performance of the five-layer device to the addition of the AlAsSb electron blocking barrier.

Figure 4 shows the low temperature light–current–voltage (L–I–V) measurements of the single- and five-layer devices whose EL spectra are shown in Fig. 3. For detailed electrical characterization, see the supplementary material. Upper hemisphere power was calculated by measuring the power of the In(Ga)Sb QD emission and integrating over an upper hemisphere of emission, assuming a Lambertian emitter. For the single-layer device, a long pass 3.6 μm filter was used to significantly reduce any contribution from the InAs host matrix. Emission from the single-layer devices appeared to saturate at low current densities, whereas the emission from the five-layer device showed nearly linear behavior across the entire range of our current source. The saturation of the single-layer device was believed to be a result of

Published under license by AIP Publishing

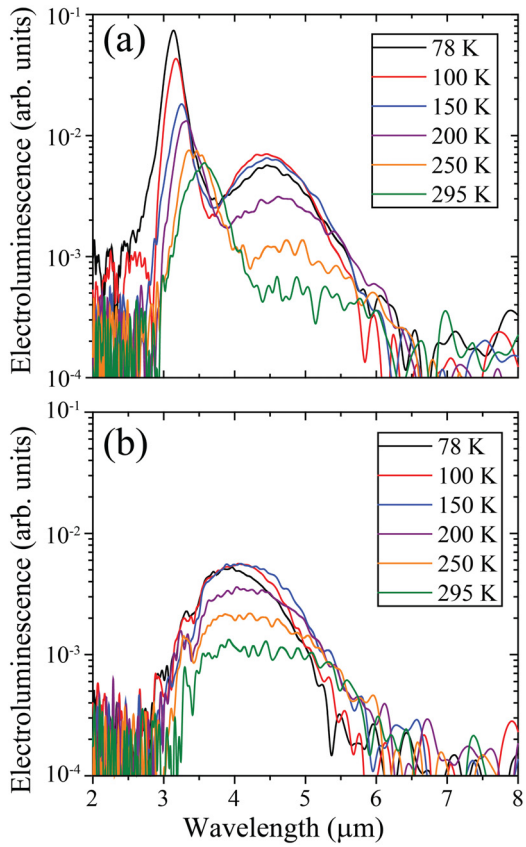

FIG. 3. Temperature-dependent EL spectrum of the (a) single-layer LED and the (b) five-layer device with AlAsSb cladding. For temperature-dependent measurements, the sample was pulsed at 400 mA in "quasi-DC" mode (a duty cycle of 50%) with a repetition rate of 10 kHz.

the limited density of QD states in the single-layer. The five-layer device, in addition to its improved temperature performance, offered a 5× increase in QD states and thus was less susceptible to the emission saturation that was observed in the single-layer device. Emission from

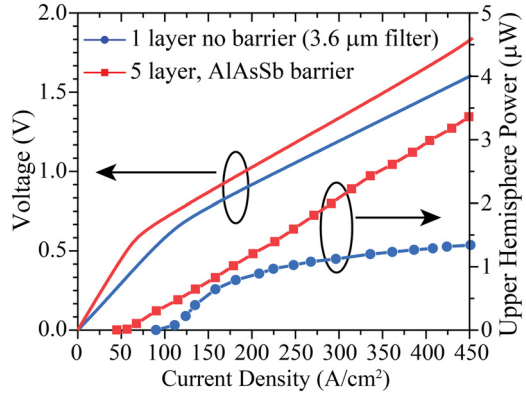

FIG. 4. L–I–V Characteristics of the single-layer (blue) and five-layer (red) devices at 78 K.

the five-layer LED showed up to 200 nW of collected power (calculated to be >3μW of power emitted to the upper hemisphere), limited only by the output of the current source and the number of wire bonds that could be contacted to a single mesa.

While the In(Ga)Sb devices presented in this paper are still susceptible to Auger recombination because of the narrow bandgap of the surrounding InAs matrix, the temperature performance of the five-layer In(Ga)Sb QD LED has distinct advantages when compared to other mid-IR LED material systems and device designs.[30–33] As a representative example, InAsSb/InAsSbP heterostructure diodes grown by LPE, with emission centered around 4.5 μm, showed a two order of magnitude decrease in the intensity of emission as temperature was increased from 77 K to 300 K, which the authors attributed to Auger recombination in the narrow bandgap InAsSb.[31] The QD emitters presented here, however, showed less than an order of magnitude decrease in emission intensity from 77 K to 300 K. The use of QDs offers at least two distinct advantages in terms of recombination dynamics and thus emission efficiency. First, the strong confinement of the charge carriers in QDs has been shown to prevent thermal escape from QD-based emitters, resulting in improved high temperature efficiency.[34] In addition, In(Ga)Sb QD zero-dimensional density of states, as compared to the two- or three-dimensional density of states in similar mid-IR LEDs, has been demonstrated to result in a significant decrease in Auger recombination,[35] which will directly impact the temperature performance of QD-based mid-IR LEDs.

We have demonstrated the utility of type-II In(Ga)Sb QDs and offered them as a potential emitter in the mid-IR. A key technology missing in the mid-IR is a simple, efficient, and room temperature LED. Available devices in this wavelength range are hampered by inefficiency in spontaneous emission operation and poor temperature performance. Because of the excellent temperature performance of the In(Ga)Sb QDs and the integration of carrier blocking layers, we demonstrated room temperature electroluminescence from a five-layer device. Future work will focus on improving the active region by optimizing the number of In(Ga)Sb layers and their dot density as well as improving hole confinement through the addition of AlInAsSb cladding layers at the anode and cathode. Previous work has demonstrated that the peak PL emission wavelength can be tuned from 4–6 μm by varying the amount of In(Ga)Sb deposited in the active region.[28] By taking advantage of this fact, it would be possible to produce separate devices that span a large portion of the mid-IR.

See the supplementary material for more details on device fabrication, photoluminescence, and electroluminescence characterization and further electrical characterization of the LEDs.

The authors gratefully acknowledge support from the National Science Foundation (No. ECCS-1926187) and Air Force Office of Scientific Research (No. AF18A-T017).

REFERENCES

[1]J. Faist, F. Capasso, C. Sirtori, D. L. Sivco, A. L. Hutchinson, and A. Y. Cho, Electron. Lett. **32**, 560 (1996).
[2]M. Razeghi, IEEE J. Sel. Top. Quantum Electron. **15**, 941 (2009).
[3]N. Bandyopadhyay, Y. Bai, S. Tsao, S. Nida, S. Slivken, and M. Razeghi, Appl. Phys. Lett. **101**, 241110 (2012).
[4]J. Faist, Appl. Phys. Lett. **90**, 253512 (2007).

Published under license by AIP Publishing

[5]L. J. Olafsen, E. H. Aifer, I. Vurgaftman, W. W. Bewley, C. L. Felix, J. R. Meyer, D. Zhang, C.-H. Lin, and S. S. Pei, Appl. Phys. Lett. **72**, 2370 (1998).
[6]W. W. Bewley, C. L. Canedy, C. S. Kim, M. Kim, C. D. Merritt, J. Abell, I. Vurgaftman, and J. R. Meyer, Opt. Express **20**, 3225 (2012).
[7]C.-H. Lin, R. Q. Yang, D. Zhang, S. J. Murry, S. Pei, A. A. Allerman, and S. R. Kurtz, Electron. Lett. **33**, 598 (1997).
[8]R. Q. Yang, C.-H. Lin, S. J. Murry, S. S. Pei, H. C. Liu, M. Buchanan, and E. Dupont, Appl. Phys. Lett. **70**, 2013 (1997).
[9]D. Zhang, E. Dupont, R. Q. Yang, H. C. Liu, C.-H. Lin, M. Buchanan, and S. S. Pei, Opt. Express **1**, 97 (1997).
[10]L. Shterengas, R. Liang, G. Kipshidze, T. Hosoda, S. Suchalkin, and G. Belenky, Appl. Phys. Lett. **103**, 121108 (2013).
[11]D. Jung, S. R. Bank, and M. L. Lee, J. Opt. **19**, 123001 (2017).
[12]A. R. Adams, Electron. Lett. **22**, 249 (1986).
[13]E. Yablonovitch and E. Kane, J. Lightwave Technol. **4**, 961 (1986).
[14]P. J. A. Thijs, L. F. Tiemeijer, P. I. Kuindersma, J. J. M. Binsma, and T. V. Dongen, IEEE J. Quantum Electron. **27**, 1426 (1991).
[15]D. Lackner, O. J. Pitts, M. Steger, A. Yang, M. L. W. Thewalt, and S. P. Watkins, Appl. Phys. Lett. **95**, 081906 (2009).
[16]P. J. P. Tang, H. Hardaway, J. Heber, C. C. Phillips, M. J. Pullin, R. A. Stradling, W. T. Yuen, and L. Hart, Appl. Phys. Lett. **72**, 3473 (1998).
[17]P. J. Carrington, V. A. Solov'ev, Q. Zhuang, A. Krier, and S. V. Ivanov, Appl. Phys. Lett. **93**, 091101 (2008).
[18]R. M. Biefeld, A. A. Allerman, S. R. Kurtz, and K. C. Baucom, J. Cryst. Growth **195**, 356 (1998).
[19]J. R. Meyer, C. L. Felix, W. W. Bewley, I. Vurgaftman, E. H. Aifer, L. J. Olafsen, J. R. Lindle, C. A. Hoffman, M.-J. Yang, B. R. Bennett, B. V. Shanabrook, H. Lee, C.-H. Lin, S. S. Pei, and R. H. Miles, Appl. Phys. Lett. **73**, 2857 (1998).
[20]W. W. Bewley, J. R. Lindle, C. S. Kim, M. Kim, C. L. Canedy, I. Vurgaftman, and J. R. Meyer, Appl. Phys. Lett. **93**, 041118 (2008).
[21]Y. Arakawa and H. Sakaki, Appl. Phys. Lett. **40**, 939 (1982).
[22]F. Hatami, M. Grundmann, N. N. Ledentsov, F. Heinrichsdorff, R. Heitz, J. Böhrer, D. Bimberg, S. S. Ruvimov, P. Werner, V. M. Ustinov, P. S. Kop'Ev, and Z. I. Alferov, Phys. Rev. B. **58**, 10064 (1998).
[23]S. Ghosh, P. Bhattacharya, E. Stoner, J. Singh, H. Jiang, S. Nuttinck, and J. Laskar, Appl. Phys. Lett. **79**, 722 (2001).
[24]N. N. Ledentsov, M. Grundmann, F. Heinrichsdorff, D. Bimberg, V. M. Ustinov, A. E. Zhukov, M. V. Maximov, Z. I. Alferov, and J. A. Lott, IEEE J. Sel. Top. Quantum Electron. **6**, 439 (2000).
[25]S. Fathpour, Z. Mi, P. Bhattacharya, A. R. Kovsh, S. S. Mikhrin, I. L. Krestnikov, A. V. Kozhukhov, and N. N. Ledentsov, Appl. Phys. Lett. **85**, 5164 (2004).
[26]D. Bimberg and U. W. Pohl, Mater. Today **14**, 388 (2011).
[27]F. Hopfer, A. Mutig, G. Fiol, M. Kuntz, V. A. Shchukin, V. A. Haisler, T. Warming, E. Stock, S. S. Mikhrin, I. L. Krestnikov, D. A. Livshits, A. R. Kovsh, C. Bornholdt, A. Lenz, H. Eisele, M. Dahne, N. N. Ledentsov, and D. Bimberg, IEEE J. Sel. Top. Quantum Electron. **13**, 1302 (2007).
[28]L. Yu, Y. Zhong, S. Dev, and D. Wasserman, J. Vac. Sci. Technol., B **35**, 02B101 (2017).
[29]E. M. Lysczek, S. E. Mohney, and T. N. Wittberg, Electron. Lett. **39**, 1866 (2003).
[30]X. Y. Gong, H. Kan, T. Makino, T. Iida, K. Watanabe, Y. Z. Gao, M. Aoyama, N. L. Rowell, and T. Yamaguchi, Jpn. J. Appl. Phys., Part 1 **39**, 5039 (2000).
[31]S. Kim, M. Erdtmann, D. Wu, E. Kass, H. Yi, J. Diaz, and M. Razeghi, Appl. Phys. Lett. **69**, 1614 (1996).
[32]A. Krier, V. V. Sherstnev, and H. H. Gao, J. Phys. D: Appl. Phys. **33**, 1656 (2000).
[33]M. J. Pullin, H. R. Hardaway, J. D. Heber, C. C. Phillips, W. T. Yuen, R. A. Stradling, and P. Moeck, Appl. Phys. Lett. **74**, 2384 (1999).
[34]A. Lévesque, P. Desjardins, R. Leonelli, and R. A. Masut, Phys. Rev. B **83**, 235304 (2011).
[35]T. Zabel, C. R. Hedlund, O. Gustafsson, A. Karim, J. Berggren, Q. Wang, C. Ernerheim-Jokumsen, M. Soldemo, J. Weissenrieder, M. Götelid, and M. Hammar, Appl. Phys. Lett. **106**, 013103 (2015).

Published under license by AIP Publishing